

Prostaglandin E₂ as transduction enhancer affects competitive engraftment of human hematopoietic stem and progenitor cells

Valentina Poletti,^{1,2,3} Annita Montepeloso,² Danilo Pellin,² and Alessandra Biffi^{1,2,3}

¹Division of Pediatric Hematology, Oncology and Stem Cell Transplantation, Woman's and Child Health Department, University of Padova, 35128 Padova, Italy; ²Gene Therapy Program, Boston Children's Dana-Farber Cancer and Blood Disorder Center, Boston, MA 02115, USA; ³Pediatric Research Institute Città Della Speranza, 35127 Padova, Italy

Ex vivo gene therapy (GT) is a promising treatment for inherited genetic diseases. An ideal transduction protocol should determine high gene marking in long-term self-renewing hematopoietic stem cells (HSCs), preserving their repopulation potential during *in vitro* manipulation. In the context of the improvement of a clinically applicable transduction protocol, we tested prostaglandin E₂ (PGE₂) as a transduction enhancer (TE). The addition of PGE₂ shortly before transduction of human CD34⁺ cells determined a significant transduction increase in the *in vitro* cell progeny paralleled by a significant reduction of their clonogenic potential. This effect increased with the duration of PGE₂ exposure and correlated with an increase of CXCR4 expression. Blockage of CXCR4 with AMD3100 (plerixafor, Mozobil) did not affect transduction efficiency but partially rescued CD34⁺ clonogenic impairment *in vitro*. Once transplanted *in vivo* in a competitive repopulation assay, human CD34⁺ cells transduced with PGE₂ contributed significantly less than cells transduced with a standard protocol to the repopulation of recipient mice, indicating a relative repopulation disadvantage of the PGE₂-treated CD34⁺ cells and a counter-selection for the PGE₂-treated cell progeny *in vivo*. In conclusion, our data indicate the need for risk/benefit evaluations in the use of PGE₂ as a TE for clinical protocols of GT.

INTRODUCTION

Prostaglandin E₂ (PGE₂) has long been investigated as a hematopoietic regulator in vertebrates, having both inhibitory and stimulatory effects depending on cell type and the timing of cell exposure.¹ The use of this molecule in experimental hematology started with the observation that short-term pulse exposure (two hours) of murine bone marrow (BM) cells to dmPGE₂ (16,16-dimethyl PGE₂), a stabilized PGE₂ molecule, enhances hematopoietic stem/progenitor cell (HSPC) homing to the marrow, as evaluated 20 h after cell injection.² Subsequent studies suggested that this phenomenon was related to a temporary increase of CXCR4 surface expression on HSPCs, favoring chemotaxis to the BM niche through the CXCR4/stromal derived-cell factor 1 axis.³ A subsequent phase I clinical study of allogeneic HSPC transplantation investigated the effects of short-term exposure to PGE₂ on human

cord blood (CB) CD34⁺ cell engraftment capability over unmanipulated CB cell batches, aiming at improving neutrophil recovery in patients.⁴ Although the study demonstrated the safety of cell treatment, it could not demonstrate a clear beneficial effect of PGE₂ stimulation on neutrophil engraftment. Despite the lack of clear effects of PGE₂ stimulation on engraftment and differentiation of human CB CD34⁺ cells, the clinical study enlightened the biopotency of PGE₂ on human HSPCs: after two hours of treatment, an upregulation of as many as ~200 genes (probe sets) involved in key biological processes such as proliferation, migration, and multiple receptors signaling was seen on the treated cells. A later extended analysis of PGE₂-treated murine hematopoietic grafts in a serial transplantation setting demonstrated that PGE₂ does not affect long-term HSPC engraftment fitness, lineage differentiation, or proliferative potential.⁵ Finally, additional studies administering PGE₂ *in vivo* in mice (by repetitive administrations) demonstrated that PGE₂ expands short-term multipotent progenitors, provides an initial enhancement of donor-cell engraftment subsequently lost in the long term in competitive transplantation assays, and ultimately does not affect long-term hematopoietic stem cell (HSC) abundance, lineage commitment, or differentiation.⁶

Recently, PGE₂ has been proposed as a lentiviral vector (LV) transduction enhancer (TE) for *ex vivo* gene therapy (GT) applications. Most TEs operate with a biochemical mechanism aimed at facilitating viral particle contact with the target cells. On the contrary, PGE₂ has a biological mechanism of action, likely happening at a post-entry level⁷ and still mostly unknown. Addition of 10 μM PGE₂ shortly before vector addition significantly increases the transduction efficiency of human HSPCs, as shown by integrated vector copy number (VCN)

Received 18 April 2023; accepted 5 October 2023;
<https://doi.org/10.1016/j.omtm.2023.101131>.

Correspondence: Valentina Poletti, Division of Pediatric Hematology, Oncology and Stem Cell Transplantation, Woman's and Child Health Department, University of Padova, 35128 Padova, Italy.
E-mail: valentina.poletti@unipd.it

Correspondence: Alessandra Biffi, Division of Pediatric Hematology, Oncology and Stem Cell Transplantation, Woman's and Child Health Department, University of Padova, 35128 Padova, Italy.
E-mail: alessandra.biffi@unipd.it



measurement on their *in vitro* progeny and, more controversially, of long-term repopulating human HSCs, as seen *in vivo* in xenotransplantation experiments.^{7–10} Moreover, recent *in vitro* data showed that LV transduction of human CD34⁺ cells with PGE2 determines a significant decrease in the abundance of the most primitive, bona fide repopulating CD34⁺/CD90⁺ HSCs within the transduced population.¹¹ All together these preclinical data may suggest that PGE2 preferentially increases the VCN of short-term progenitors rather than long-term repopulating HSCs.

PGE2 is currently used as a TE in GT clinical studies for β -hemoglobinopathies (HGB-207 and HGB-206)^{12,13} and for Hurler syndrome,¹⁴ and interim results have been recently published. In clinical studies for sickle cell disease (HGB-206) and β -thalassemia (HGB-207), investigators started the trials with an original cell manufacturing process not including TEs and then refined it by adding PGE2. By these means, the investigators obtained a significantly higher VCN in the drug products and in the patients' peripheral blood (PB) mononucleated cells at the latest follow-up.^{12,15} However, in the HGB-206 study, they observed a decrease in the frequency of high-VCN progenitors in the PB and BM patient samples compared with the infused cell product, suggesting that high-VCN progenitors may not have contributed to the engrafted gene-modified cell populations in the long term.¹⁶ In the clinical study for β -thalassemia, despite a higher VCN obtained with PGE2, investigators did not describe an overt clinical advantage compared with the original protocol.¹² In the Hurler syndrome trial, investigators similarly measured a decrease of VCN from the drug product to the BM and PB cells evaluated at two-year follow-up¹⁴ that showed VCNs comparable with those observed in patients affected by similar conditions and treated with GT products manufactured without PGE2.^{17–19} In terms of long-term engraftment, Gentner et al.¹⁴ reported ~47% of vector-positive BM-derived colony-forming cells (CFCs) at a maximal follow-up of 12 months versus an average of 55% with the original protocol lacking PGE2.¹⁹

To obtain information that could help determine the actual indication for PGE2 use in manufacturing GT products for the clinics, we investigated *in vitro*, *in vivo* (in a competitive xenotransplantation setting), and *ex vivo* the effects of PGE2 use as TE on the clonogenic potential and repopulation capacity of human mobilized PB (mPB) CD34⁺ HSPCs in comparison with cells transduced with a standard protocol not using TEs (STD).¹⁷

RESULTS

PGE2 robustly increases HSPC transduction by LVs *in vitro*, but reduces clonogenic potential of the treated cells

Human CD34⁺ cells derived from granulocyte colony-stimulating factor (G-CSF) mPB of healthy donors were mock transduced or transduced with a LV designed for the GT of neuronal ceroid lipofuscinosis (LV.PPT1co)²⁰ in STD¹⁷ or with the addition of PGE2 to the standard transduction cocktail, used with a timing and concentration previously demonstrated to enhance LV transduction (10 μ M, added two hours before transduction).⁸ To further test the effect of PGE2 on cell culture and transduction, we also anticipated its use to the time

of thawing. One or two hits of overnight transduction at a multiplicity of infection (MOI) of 100 were performed with LV.PPT1co. After each transduction, cells were washed and maintained in liquid culture as a bulk cell population for two weeks and as individual hematopoietic progenitors in semi-solid medium for a CFC assay to evaluate clonogenic potential. As expected, LV transduction efficiency, determined as the number of integrated vector copies (VCN)/cell on the 14 day liquid and semi-solid culture progeny of the transduced cells, was significantly increased by PGE2 addition 2 h before virus addition but not by a longer pre-stimulation (Figure 1A). However, transduction in the presence of PGE2 resulted in a significant reduction of the *in vitro* CD34⁺ cell clonogenic potential on CFC assay (Figure 1B). This detrimental effect of PGE2 stimulation was dependent from the duration of the stimulation and not from an over-transduction toxicity, as cells incubated with PGE2 from thawing (~40 h) produced 1/3 fewer colonies than the STD at a comparable VCN (Figure 1B).

CXCR4 antagonist I rescues the detrimental effect of PGE2 on HSPC clonogenic potential

As CXCR4 is a well-known target of PGE2 and is involved both in viral infection and stem cell biology, we investigated the effects of CXCR4 modulation in our experimental conditions. Two independent LV transductions at an MOI of 100 were performed on human CD34⁺ cells from G-CSF mPB of healthy donors. Cells were transduced in the presence or absence of PGE2, added at the thawing or two hours before transduction, with or without the addition of the CXCR4 antagonist I AMD3100 (10 μ M). Cells were analyzed for CXCR4 expression using cytofluorimetry at thawing and immediately before and after transduction (Figure 1C), when the cells were washed and plated as a bulk population in liquid culture or as individual hematopoietic progenitors in a CFC assay. At thawing, ~90% of the cells were CXCR4⁺ (Figure S1) with a mean fluorescence intensity (MFI) of approximately 800 (Figure 1C). After 24 h of pre-activation in STD, CXCR4 expression was stable, but MFI almost doubled compared with thawing when PGE2 was added to the incubation media in the 2 h before initiating transduction (Figure 1C). Cells incubated with PGE2 from thawing (PGE2long in Figure 1C) were virtually all CXCR4⁺ (Figure S1) and showed a ~6-fold higher CXCR4 expression level than the condition without PGE2. Previously published data indicate that CXCR4 antibody (clone 12G5) competes with AMD3100 for binding to CXCR4.²¹ Indeed, addition of AMD3100 to the cell samples resulted in an apparent reduction of CXCR4 expression level (Figures 1C and S1), confirming the binding of the drug to CXCR4. After the overnight transduction, cells incubated with PGE2 2 h before transduction showed a further 2.3-fold increase of CXCR4 expression, while cells incubated with PGE2 from thawing significantly downregulated it. VCN measurement on the transduced cells showed that AMD3100 did not compromise the PGE2 effect on transduction (Figure 1D). Rather, importantly, it reversed the effect of PGE2 in reducing the CD34⁺ cell clonogenic potential, as shown by the CFC assay (Figure 1E).

To confirm these observations, we evaluated the effects of PGE2 over different times of incubation. A pool of CD34⁺ cells derived from two

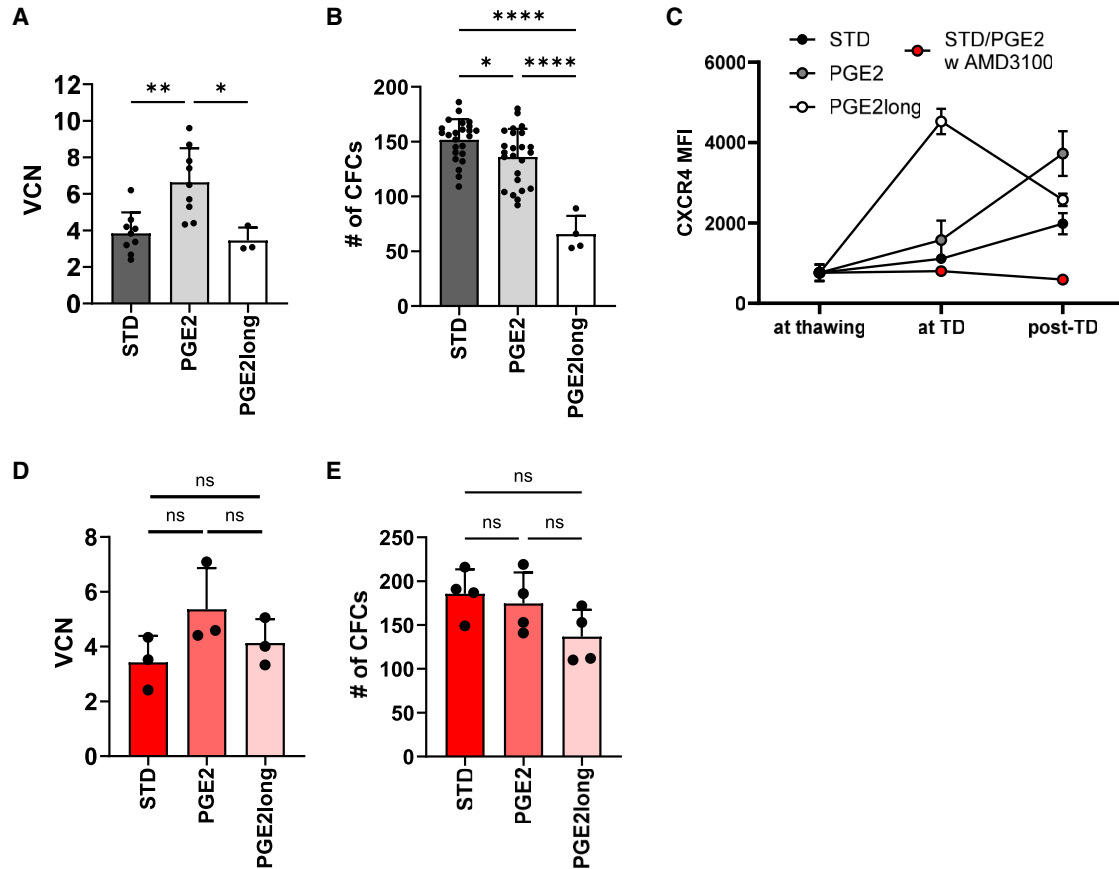


Figure 1. PGE2 increases lentiviral transduction and CXCR4 expression and reduces HSPC clonogenicity

Transduction efficiency (A) and CFC assay (B) of human CD34⁺ cells transduced with PGE2, added two hours before transduction (PGE2) or at cell thawing (PGE2long) compared with a standard condition (STD). (C) Expression level (mean fluorescence intensity) of CXCR4 in human CD34⁺ cells at thawing and before and after LV transduction with or without AMD3100, a CXCR4 antagonist. N = 3 independent experiments; mean (SD) is shown. (D) Transduction efficiency and (E) CFC assay performed in the presence of AMD3100. (A), (B), (D), and (E) refer to a single experiment performed in triplicate, with additional replicates for STD and PGE2 conditions. Mean (SD) is shown, and statistical significance was determined using one-way ANOVA with multiple pairwise comparisons (*p < 0.05, **p < 0.01, ***p < 0.001, and ****p < 0.0001; ns, not significant).

healthy donors were incubated with or without PGE2, in the presence or absence of AMD3100 and analyzed after 2, 6, 24, 36, and 48 h. We chose 48 h as the maximal incubation time consistent with the longest timing for *in vitro* cell manipulation in GT clinical transduction protocols. At each time point, we performed a CFC assay in duplicate, a cell growth curve, and a cytofluorometric analysis of CXCR4 expression. Consistent with the data above, also in this setting at each time point, including the shorter incubation of only 2 h, cells incubated with PGE2 generated significantly fewer ($p < 0.0134$, two-way ANOVA) colonies compared with cells cultured in STD (Figure 2A). As above, also in these experimental conditions, the addition of AMD3100 rescued the clonogenic potential of the PGE2-treated HSPCs. To follow the cell growth rate, 5×10^4 cells were collected at each time point and cultured for 12 days in expansion medium, counting them every other day starting from day 5 from plating. PGE2 barely affected the cell growth rate but caused significantly lower cell recovery at the end of the culture (Figure 2B), an effect that was partially rescued by concomitant AMD3100 administration.

Cytofluorimetric analysis confirmed the binding of AMD3100 to the CXCR4 receptor for the whole experiment duration as per the resulting apparent reduction of CXCR4 expression (Figure 2C).

PGE2 reduces the HSPC long-term repopulation potential

To assess whether PGE2 would have an effect not only on colony-forming progenitors but also on LT-HSCs, we evaluated the expression of HSC markers on STD vs. PGE2-treated cells using cytofluorimetry. Interestingly, this analysis revealed that among other tested markers (CD133, CD45RA, CD38, and CD90; Figure S2) the expression of CD90 was significantly reduced in the CD34⁺ cells cultured in the presence of PGE2 in comparison with cells treated with STD (Figure 3A). On the basis of this early evidence, we monitored the fate of PGE2-treated cells *in vivo*. We performed a competitive transplantation assay in immunodeficient NBSGW mice (NOD.Cg-Kit^{W-41J} Tyr⁺ Prkdc^{scid} Il2rg^{tm1Wjl}/ThomJ) that have an additional deletion in *c-Kit* compared with standard NSG mice and do not require myeloablation to support human cell engraftment.

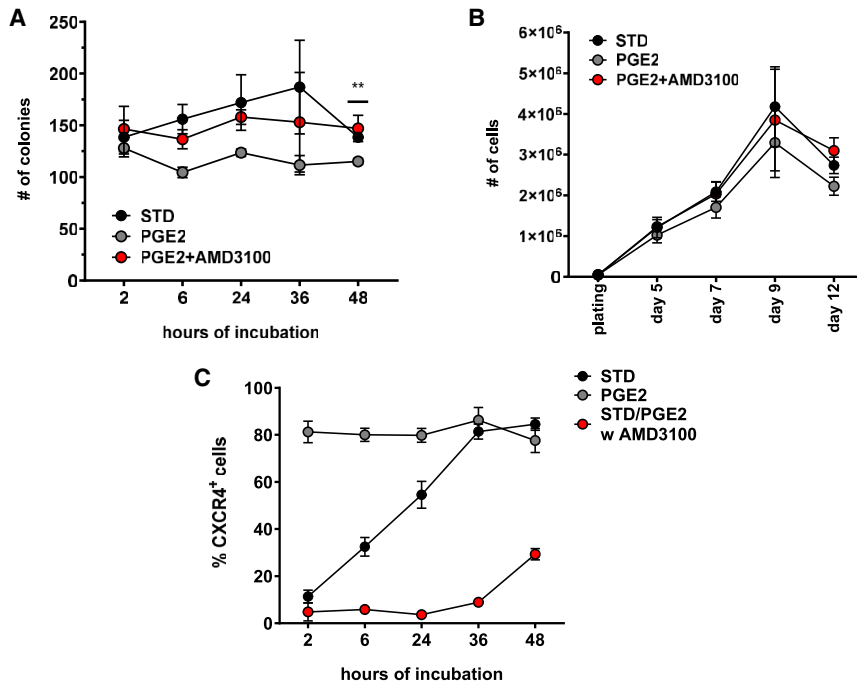


Figure 2. AMD3100 rescues the detrimental effect of prostaglandin E₂ on HSPC clonogenic potential

Time course CFC assay (A), cell growth curve (B), and percentage of CXCR4⁺ CD34⁺ cells after 2, 6, 24, 36, and 48 h of incubation with PGE₂ with or without AMD3100. Mean (SD) is reported, and statistical significance was determined using two-way ANOVA with multiple pairwise comparisons (**p < 0.01; ns, not significant). In (A), adjusted p = 0.0012 (**) between STD and PGE₂, and adjusted p = 0.0105 (*) between PGE₂ plus AMD3100 and PGE₂ were determined at 48 h.

cells transduced with PGE₂ showing the highest CXCR4 MFI (Figure S3B). Two weeks post-transduction, pools of progenitors and liquid cultures were collected to determine the transduction efficiency by cytofluorimetric analysis of GFP expression (Figure S4A) and VCN evaluation. We obtained a different transduction level in the three independent transductions, ranging from a low level in TD3 (<40% LV⁺ cells), to an intermediate level in TD1 (80%–94% LV⁺ cells), to a very high level in TD2,

with virtually all the cells transduced (Figure S4A). Consistently, average VCN value range was 0.4–1.2 in TD3 cells, 3–5 in TD1 cells, and 7–10 in TD2 cells (Figure 3C). This differential transduction efficiency was likely due to the use of CD34⁺ cells derived from different donors and multiple viral vector batches in the three TDs. The overall number of CFCs was comparable in the three cell products, except for a trend toward reduced clonogenic potential in cell samples transduced with PGE₂, as expected (Figure S4B).

After transplantation, human cell chimerism and hematopoietic composition were assessed monthly in the PB of the transplanted mice using cytofluorimetry (Figure 3D). At the end of the study mice were sacrificed, and the hematopoietic organs (BM, PB, spleen, and thymus) were collected and processed to determine human cell engraftment, VCN, and hematopoietic reconstitution. Thymi were generally poorly developed or completely absent in most of the animals. Human cell engraftment was defined as fraction of human CD45⁺ cells within murine hematopoietic cells, and we considered as engrafted mice with ≥0.1% and 1% of human CD45⁺ cells in the PB and BM, respectively. Robust human cell engraftment was measured in the hematopoietic organs (PB, BM, and spleen) of mice receiving TD1 and TD3 cells, while a variable low level was observed in mice receiving TD2 cells (Figures 3E, 4A, and 4E), possibly related to a transduction-related effect. To calculate the contribution to the human CD45⁺ cells of the STD-GFP vs. Cherry cell progeny, the GFP/Cherry ratio was determined using cytofluorimetry and compared with the actual cell ratio at the infusion on the basis of the precise percentage of GFP⁺ and Cherry⁺ cells in each cell product. Interestingly, for all the tested organs, the GFP/Cherry ratio remained unchanged in the reference groups A and B,

We used this murine model to investigate the cell-intrinsic engraftment capability of human HSPCs transduced with or without PGE₂, in the absence of additional signals deriving from a conditioned BM niche possibly modulating cell homing or engraftment. Three independent transductions (TD1, TD2, and TD3) were performed on human mPB CD34⁺ cells derived from four healthy donors (TD1 and TD2 corresponded to two individual donors, while TD3 cells were derived from a pool of two different donors) with multiple viral vector batches. Cells were thawed, pre-activated for 24 h, and transduced overnight in STD or in the presence of PGE₂ with or without AMD3100 added two hours before transduction, with an LV expressing a green (GFP) or a red (Cherry) monomeric fluorescent protein. After ~40 h of *in vitro* culture inclusive of transduction, cells were collected, washed, counted, and immediately transplanted intravenously in NBSGW mice according to a competitive design. In particular, each recipient mouse received a total of 3 × 10⁵ CD34⁺ cells by intravenous injection, 50% of which were transduced with LV.GFP in STD condition and 50% with LV.Cherry in STD condition (control group A, N = 7), with the addition AMD3100 (control group B, N = 8), with the addition of PGE₂ two hours before transduction (group C, N = 8), or with PGE₂ plus AMD3100 added two hours before transduction (group D, N = 8). Three additional control groups included untreated (UT) mice (N = 3) or animals transplanted in a non-competitive setting, receiving 3 × 10⁵ CD34⁺ cells transduced with LV.GFP in STD (group E, N = 3) or with PGE₂ (group F, N = 3), respectively (Figure 3B). Part of the cells were used for a cytofluorimetric analysis of CD34 and CXCR4 expression, maintained in liquid culture as a bulk population, or plated as individual progenitors for a CFC assay. At transplantation, virtually all the cells were CD34⁺ (Figure S3A), and ≥80% of the cells were CXCR4⁺, with

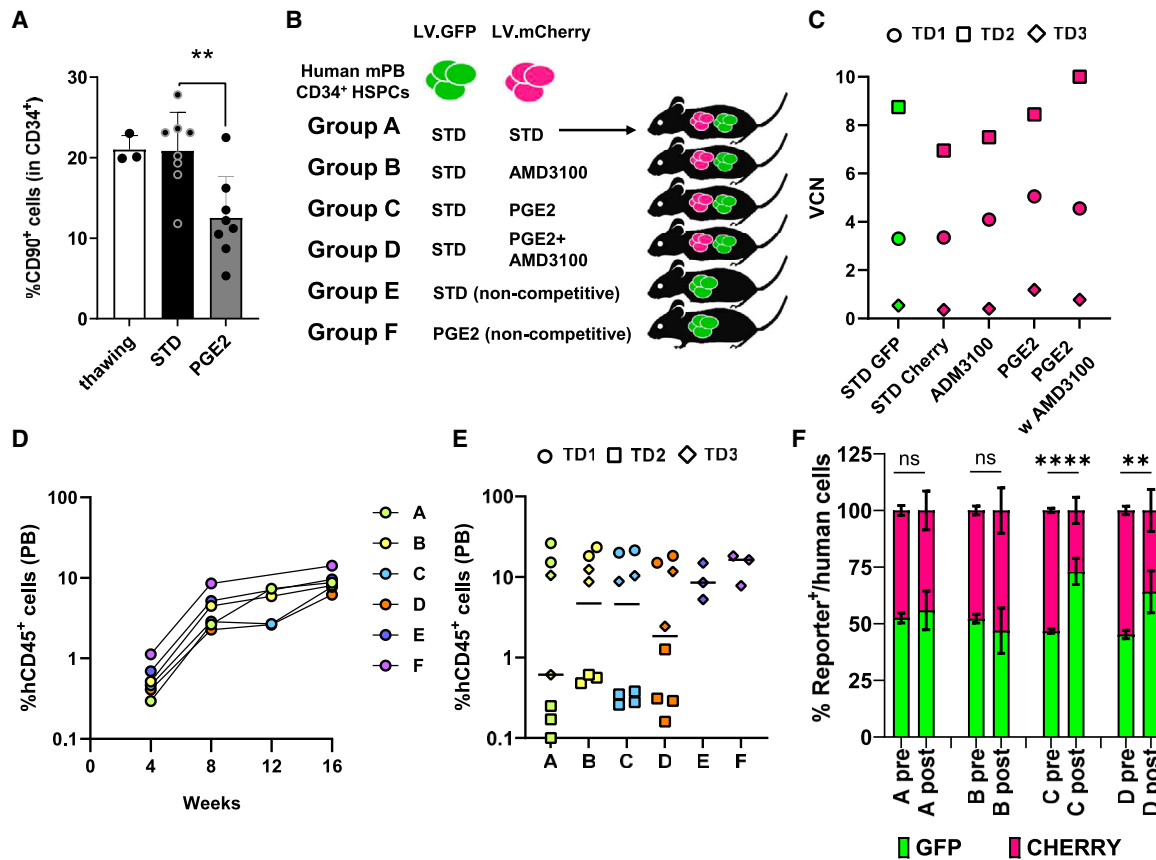


Figure 3. Competitive transplantation of human HSPC transduced with PGE2 in NBSGW mice

(A) Fraction of primitive $CD90^+CD34^+$ cells at thawing and after transduction with or without PGE2; mean (SD) is reported with statistical significance calculated using unpaired t test (** $p < 0.01$). (B) Scheme of the *in vivo* study: human $CD34^+$ cells were transduced with an LV expressing GFP or mCherry with or without PGE2 and transplanted in competitive or non-competitive setting into immunodeficient NBSGW mice. (C) Vector copy numbers obtained in the *in vitro* liquid culture of the three transduced cell batches (TD1, TD2, and TD3) two weeks post-transduction. (D) Human cell chimerism (mean only) in the peripheral blood of transplanted mice over time, determined as fraction of human $CD45^+$ cells. Human cell chimerism (E) and GFP⁺/Cherry⁺ (F) cell composition in the peripheral blood of individual mice at sacrifice. In (E), median is reported, while in (F) mean (SD) is reported, and statistical significance was calculated using the χ^2 test with Yates's correction (ns, not significant; ** $p < 0.01$ and **** $p < 0.0001$).

while a significant relative reduction of Cherry⁺ cells, transduced with PGE2, was observed in mice of group C in favor of the STD-GFP cell compartment (Figures 3F, 4B, and 4F). AMD3100 addition (group D) only partially rescued the PGE2 effect in the PB and in the spleen (Figures 3F and 4F). A human CFC assay performed on the total BM cells at sacrifice resulted in a comparable number of human progenitors in all the groups, with fewer colonies obtained from the BM of mice receiving TD2 cells, characterized by the highest VCN values, as in the infused cell product (Figure S5A). In the BM of transplanted mice, the composition of human hematopoietic cells in the different lineages remained substantially unchanged, with most of the cells showing a B lymphoid (40%–80%) and myeloid (20%–25%) phenotype (Figure S5B). Measurement of the VCN of the human cells engrafted in the mice (BM and BM-derived colonies, Figures 4C and 4D) showed values consistent with those detected in the infused cell products.

LV integration profile in human NBSGW-repopulating cells derived from $CD34^+$ transduced with PGE2

The LV integration pattern in the cells transduced in the presence of PGE2 was investigated *in vitro* in human $CD34^+$ cells (TD1 cells) and *in vivo* in the sorted GFP⁺ and Cherry⁺ cells collected from the BM of four representative mice receiving TD1 cells, i.e., mice #A2_1 and #A2_3 (group A) and mice #C1_1 and #C1_2 (group C) (Figure 5A). The aim of the analysis was to detect any possible alteration of the normal LV integration pattern related to PGE2 stimulation, i.e., an unusual set of LV-targeted genes or an unexpected clonal abundance, skewing, or selection happening *in vivo*, taking advantage of the LV integration as a genetic marker of the original repopulating HSCs. LV integration sites (ISs) were recovered by ligation-mediated PCR (LM-PCR) followed by high-throughput Illumina sequencing, as previously described,²² followed by established bioinformatic processing including a step

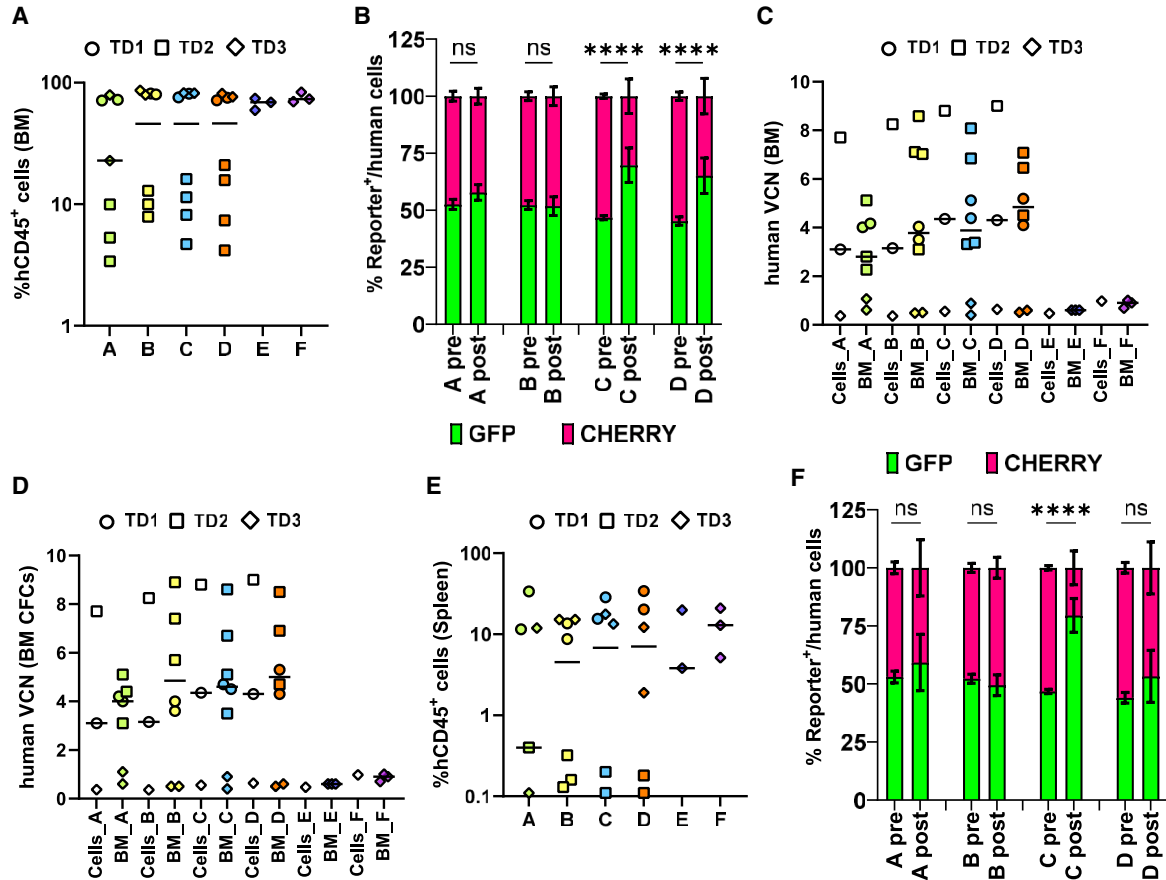


Figure 4. PGE2 reduces the HSPC long-term repopulation potential

Human cell chimerism (A) and GFP⁺/Cherry⁺ (B) cell composition in the bone marrow of individual mice at sacrifice. Human-cell VCN calculated in the total BM cells at sacrifice (C) and in the pool of human CFCs derived from the BM of individual mice (D). Human cell chimerism (E) and GFP⁺/Cherry⁺ (F) cell composition in the spleen of the transplanted mice at sacrifice. In (A), (C), (D), and (E), the median is shown. In (B) and (F), mean (SD) is shown, and statistical significance was calculated using the χ^2 test with Yates's correction (ns, not significant; **** $p < 0.0001$).

of collision/contamination filtering.¹⁷ We obtained 7,789 and 5,477 univocal ISs mapped on the human genome (National Center for Biotechnology Information [NCBI] Hg38) in TD1-STD and TD1-PGE2 cell samples, respectively. To increase the strength of our comparative analysis, we included an additional sample of CD34⁺ cells transduced with PGE2 (TD2-PGE2) including 13,506 ISs and a large reference dataset of 67,884 ISs previously retrieved by multiple samples of G-CSF mPB CD34⁺ HSPCs transduced in STD with clinically relevant LVs (CCL-SIN-18-WPRE backbone).^{22,23} To build an *in vivo* IS dataset, BM mononucleated cells of mice A2_1 and A2_3 and C1_1 and C1_2 were sorted for GFP and Cherry using a fluorescence-activated cell sorter immediately after sacrifice. Approximately 1 million GFP⁺ and Cherry⁺ cells were obtained with a >99% of purity. Genomic DNA (gDNA) was extracted and used for VCN determination and LM-PCR. The resulting VCNs were consistent with the infused cells, with relatively higher VCN values observed in PGE2-Cherry⁺ cells of group C mice (Table S1).

We did not observe a different genomic IS distribution than expected either *in vitro* and *in vivo*, with most of the LV integrations targeting gene introns and the fraction of intergenic ISs increasing *in vivo* (~29%) with respect to the cultured CD34⁺ cells (18%) (Figure 5B), suggesting an *in vivo* counter-selection for intragenic integrations already observed in other preclinical studies.^{22,24} Seventy percent of the target genes identified in CD34⁺ cells transduced with PGE2 were already identified as preferential targets of LV integration and included in our large reference dataset of 67,000 ISs covering 9,304 genes (Figure S6A). A biological function analysis performed by Gene Ontology Enrichment software²⁵ revealed no difference in the TD1-STD and TD1-PGE2 target gene lists (Figure 5C), with most of the enriched functional categories related to nucleic acid and protein metabolism, cell organization, and immune response. Among the 104 top 1% most targeted genes in PGE2 cell samples (TD1 + TD2), 30 genes were already identified as well-known preferential LV target genes described in multiple preclinical^{22–24} and clinical^{17,26–28} studies (e.g., *DACH1*, *FANCA*, *FCHSD2*, *KDM2A*, *NPLOC4*, *PACS1*). A word

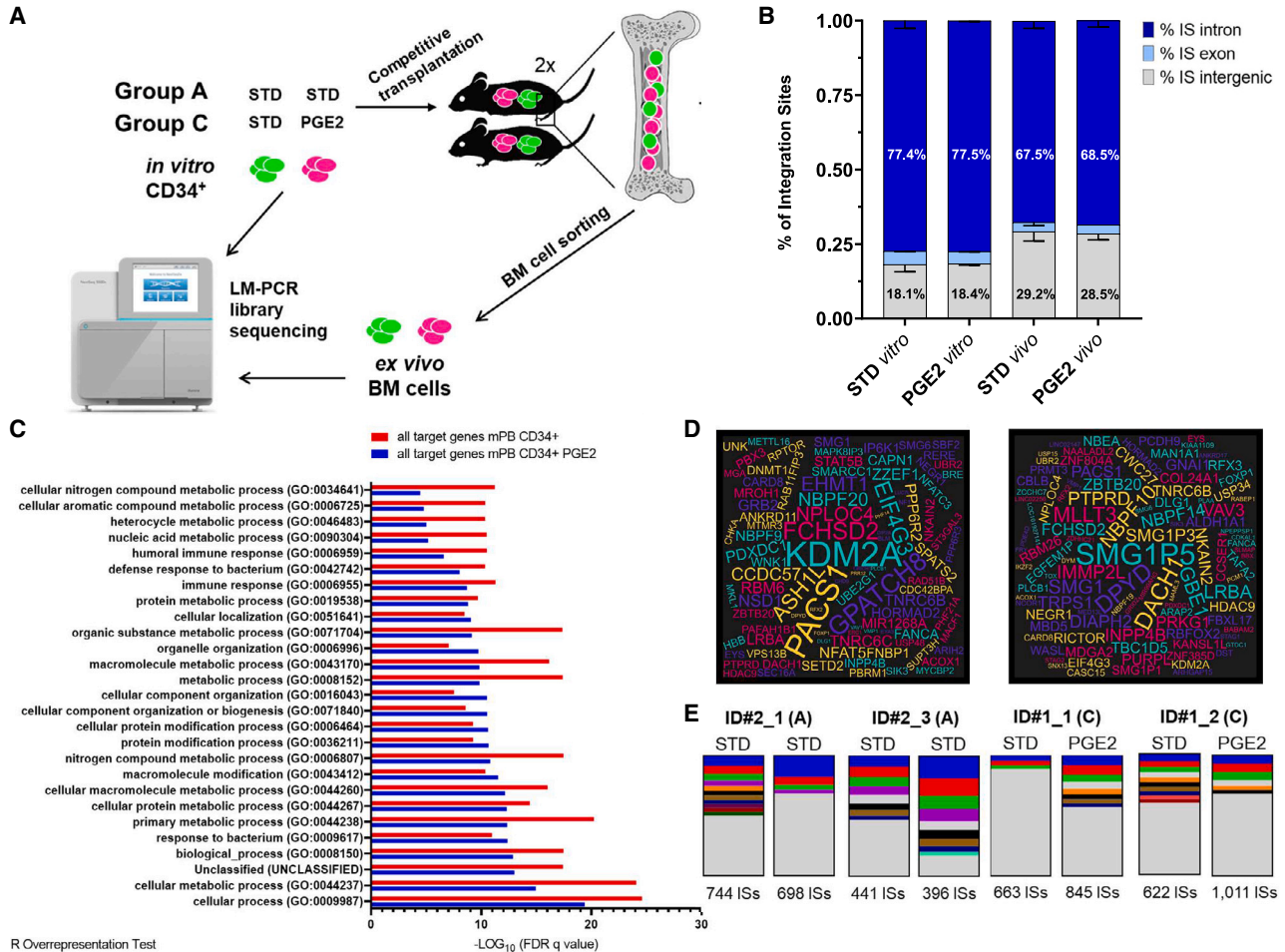


Figure 5. PGE2 does not alter the canonical lentiviral vector integration profile in human HSPCs

(A) Schematic view of the lentiviral vector integration site analysis. (B) Genomic distribution of the vector integration sites in analyzed cell samples; mean (SD) is shown. (C) Gene Ontology categories significantly enriched in the list of LV-target genes in the *in vitro* progeny of transduced CD34⁺ cells. (D) Word cloud graph showing the top 1% LV target genes in the *in vitro* progeny of CD34⁺ cells transduced in standard conditions (left) and with PGE2 (right); the color of the words is random, while their size is proportional to the relative integration frequency. (E) Histogram plots representing individual cell clones with a read count greater (colored) or lower than 3% of total reads, retrieved in the sorted GFP⁺ or Cherry⁺ BM cells of the individual analyzed mice.

cloud graph showing the top 1% LV target genes in CD34⁺ cells transduced in standard (left) and with PGE2 (right) is shown in Figure 5D.

From the BM GFP⁺ and Cherry⁺ cells we obtained ~400 to 1,000 unique ISs in each individual sample. The overall fraction of original reads accounting for a particular IS was used as a surrogate readout of the relative abundance of a cell clone harboring a particular integration. Almost every IS-marked cell clone accounted for only a small fraction of the total clones, similarly in the STD and PGE2 BMs, with only a few clones occasionally accounting for >3% of the reads (Figure 5E), without any evidence of clonal recurrence in different samples. By an enrichment pathway analysis performed with Reactome²⁹ on the genes targeted in the most abundant cell clones, no pathway resulted significant enriched after multiple comparison correction (Tables S2 and S3).

We finally assessed the occurrence of LV integration bias for known oncogenes at the time of transduction or an *in vivo* selection of clones harboring integrations in oncogenes, which may potentially confer growth advantage. As a result, no difference in the percentage of target oncogenes was found in the CD34⁺ cell progeny either *in vitro* (14% STD and 13% PGE2; Figure S6B) and *in vivo*, where 13%–18% of the most abundant cell clones carried insertions in known oncogenes, independently from the transduction conditions (Figure S6C). From these results we concluded that no alterations in the normal LV integration pattern, gene selection, or clonal dominance events occurred in CD34⁺ cells transduced with PGE2 and in their *in vivo* progeny.

DISCUSSION

The ideal HSPC transduction protocol for GT applications minimizes cell manipulation; preserves the cell clonogenic potential, engraftment

capability, and multi lineage repopulation ability; and allows an adequate VCN in long-term repopulating HSCs. PGE2, a powerful bioactive lipid, has been proposed as a promising molecule first to increase human HSPC engraftment ability, then as lentiviral TE. Although it has been extensively demonstrated that PGE2 addition to media used for LV-mediated transduction of human CD34⁺ cells efficiently increases the lentiviral VCN measured on their *in vitro* progeny in multiple preclinical^{7–10} and clinical studies,^{12,14,15} it remains debated if a solid transduction advantage is seen also on long-term repopulating HSCs.¹⁶

Our study was conducted as part of transduction protocol optimization efforts for clinical application of HSC GT and was focused mainly on the potential effects of PGE2 used as TE in a single-hit version of a transduction protocol successfully used in multiple previous clinical studies.^{17,26} After transducing mPB CD34⁺ cells in the presence or absence of PGE2, we investigated the long-term effects of PGE2 on the transduced cell *in vitro* clonogenic potential and on the *in vivo* repopulation capacity by a competitive repopulation assay in humanized immunodeficient mice. As expected, lentiviral transduction with PGE2 significantly increased the VCN of the CD34⁺ myeloid cell progeny *in vitro*. Concomitantly, however, transduction with PGE2 significantly reduced the cell clonogenic potential with respect to cells transduced without PGE2. Although a higher VCN was obtained only when PGE2 was administered two hours before transduction (and not since thawing), the impairment of the HSPC clonogenic potential was of increasing severity at prolongation of PGE2 exposure. Interestingly, a time-dependent significant increase in CXCR4 surface expression was noticed in cells exposed to PGE2. These findings let us hypothesize the existence of a potential correlation between CXCR4 overexpression and transduction efficiency. By co-administering PGE2 and AMD3100, a powerful CXCR4 inhibitor, we demonstrated the absence of such a correlation. However, we noticed that co-administration of AMD3100 with PGE2 allowed preserving CD34⁺ cell clonogenicity.

Actually, AMD3100 addition alone to the culture medium increased the number of colonies in the CFC assay, even compared with the STD protocol. This observation may suggest that a fine-tune regulation of the levels of CXCR4 surface expression is key for the maintenance of a physiological HSPC homeostasis, as its dramatic and sustained overexpression could be detrimental to this process. Notably, reduction of CXCR4 expression^{30,31} has been associated to enhanced BM engraftment of human HSCs.^{30,31}

In the *in vivo* study, mPB CD34⁺ cells from multiple donors were transduced overnight with or without PGE2 with an LV expressing GFP (STD) or Cherry (PGE2), and competitively transplanted (fifty-fifty) in humanized NBSGW mice. By testing cell products at increasing VCN (low, intermediate, and very high), we could discriminate the effects of a high VCN/transduction level alone from the PGE2-specific effects. Four months post-transplantation, all animals showed a satisfying human cell chimerism in the BM (>80%) except the animals that received the cell product with the highest VCN (TD2;

average VCN ~ 9), likely an effect of over-transduction. Independently from the overall human cell chimerism, we noticed that the GFP/Cherry cell composition of the BM, PB, and spleen was in favor of the GFP⁺ cell compartment, suggesting that in a challenging competitive setting, CD34⁺ cells transduced in the presence of PGE2 could be disadvantaged in engraftment and/or long-term repopulation of the host. This evidence was confirmed in the peripheral hematopoietic organs, namely, PB and spleen. This observation is in line with the significant reduction of primitive CD34⁺/CD90⁺ HSCs that we, and other investigators,¹¹ detected by cytofluorimetric analysis following PGE2 exposure. Differently from what observed *in vitro* at CFC assay, temporary blockage of CXCR4 by AMD3100 administration did not rescue the PGE2-mediated repopulation disadvantage *in vivo*, supporting the hypothesis that this latter phenomenon is likely due also to additional/more complex cell alterations. Interestingly, cells transduced in the presence of AMD3100 were able to repopulate NGSBW mice (group B mice in the study) as cells transduced in STD. This finding is in line with the data produced by Kollet et al.³² showing efficient NSG repopulation with CXCR4^{-/low} human CD34⁺ HSPCs, describing a finely regulated turnover between its intracellular and surface expression. Notably, mice receiving CD34⁺ cells transduced STD or with PGE2 and transplanted in a non-competitive setting, showed a comparable, high human cell chimerism (~80%). Thus, these data confirm an overall still acceptable safety of the transduction with PGE2 but highlight a limited, but existing, relative repopulation disadvantage associated to the cell treatment that is exacerbated by a competitive and challenging setting. High VCN values may synergistically contribute to this phenomenon, as a repopulation unbalance in favor of STD-GFP⁺ cells was observed only in mice receiving cells VCN>3 (TD1 and TD2), not in mice receiving TD3 cell product (VCN < 1). However, in mice receiving TD2, transduced at saturation both with and without PGE2 (VCN ~ 9), STD-GFP cells gave the greatest contribution to BM repopulation (>90% of total human cells), suggesting overall better fitness. We may thus speculate that LV transduction in the presence of PGE2 may have triggered cellular alterations, likely at genetic or epigenetic level, of HSPCs that could have affected their clonogenic potential *in vitro* and their repopulation capacity *in vivo*. Of note, by analyzing the LV integration characteristics in CD34⁺ cells transduced with PGE2 *in vitro* and in their repopulating progeny *in vivo*, we did not observe any substantial alteration with respect to the usual LV integration pattern and target gene set.

Overall, considering the significant reduction of CD34⁺ cell clonogenic potential *in vitro*, the relative repopulation disadvantage of cells transduced with PGE2, and the sustained alteration of CXCR4 expression with unknown long-term consequences, we did not conclude in favor of a modification of our current transduction protocol with the addition of PGE2.

MATERIALS AND METHODS

Human cell culture and transduction

Human CD34⁺ cells from healthy donors were purchased from AllCells. After thawing, cells were pre-activated for 24 h in GMP

SCGM medium (CellGenix) added of a human recombinant cytokines cocktail (PeproTech, Inc.), as previously published.¹⁷ Three hundred thousand cells were transduced overnight in the same medium (defined as STD) at an MOI of 100. PGE2 (MP Biomedicals) and/or AMD3100 (Merck Millipore Calbiochem) was added in the culture medium 2 h before transduction (or at thawing when indicated) at a concentration of 10 μ M. Cells were transduced with a therapeutic SIN LV³³ or an equivalent LV carrying a gene encoding a GFP or Cherry protein under the transcriptional control of the human phosphoglycerate kinase gene (*PGK*) promoter. After transduction, cells were washed and maintained in liquid culture in Iscove's modified Dulbecco's medium (IMDM; Sigma-Aldrich) with fetal bovine serum (10%; Gibco-Thermo Fisher Scientific) and human SCF (0.3 μ g/mL), IL-3 (0.06 μ g/mL), and IL-6 (0.06 μ g/mL) cytokines (all PeproTech Inc.). CFC assay from CD34⁺ cells was performed by plating 1,000 cells/mL of MethoCult H4435 Enriched medium (STEMCELL Technologies Inc.) in duplicate. CFC assay from total BM cells was performed by plating 150,000 cells/mL of MethoCult after erythrocytes lysis with ACK (ammonium-chloride-potassium) buffer (ammonium chloride 8,290 mg/L, potassium bicarbonate 1,000 mg/L, and EDTA 37 mg/L). Two weeks later, colonies were counted and collected as a pool for gDNA extraction, together with cells maintained in liquid culture. gDNA extraction was performed with DNeasy Blood & Tissue Kit (QIAGEN). gDNA (20 ng) was used for VNC determination by duplex digital droplet PCR (BioRad) following the manufacturer's instructions, with specific primers annealing on the viral *Psi* (forward sequence: TGAAAGCGAAAGGGAAACCA; reverse sequence: CCGTGCGCGCTTCAG; probe sequence: AGCTCTCTCGACGCAGGACTC) and on the human *ALB* gene as a reference (forward sequence: GCTGTCATCTCTTGTGGGCTGT; reverse sequence: ACTCATGGGAGCTGCTGGTTC; probe sequence: CCTGTCATGCCACACAAATCTCTCC).

Transplantation of human cells

Six to 8-week-old female NBSGW mice (stock #026622)³⁴ were purchased from Jackson Laboratory (Bar Harbor, ME) and maintained at the Dana-Farber Cancer Institute animal research facility. Procedures involving animals and their care were conducted in conformity with the institutional guidelines according to the international laws and policies (NIH Guide for the Care and Use of Laboratory Animals, U.S. National Research Council, 1996). The specific protocols covering the studies described in this paper (15-031) were approved by the Dana-Farber Cancer Institute Animal Care and Use Committee. After 24 h of pre-activation and an overnight transduction (for a total of ~40 h of *in vitro* culture), human CD34⁺ cells transduced with LV-GFP or LV-Cherry were washed, counted, pooled fifty-fifty in a total of 3 \times 10⁵ cells in 100 μ L PBS, and immediately injected in mouse tail vein. Mice were maintained for 16 weeks post-transplantation, and blood collection was performed at 4, 8, and 12 weeks and at sacrifice for evaluating human cell chimerism and composition by cytofluorimetric analysis. At sacrifice, mice were euthanized under deep anesthesia. BM, spleen, and thymus were collected and differentially processed. BM cells were collected by flushing the femurs with PBS 2% FBS. Spleen and

thymus cells were mechanically disaggregated to obtain a single-cell suspension in PBS 2% FBS.

Flow-cytometric analysis

For cytofluorimetric analysis of stem and progenitor composition of human CD34⁺ cells cultured in STD conditions or in the presence of AMD3100 and PGE2, 1 \times 10⁵ cells were suspended in blocking solution (PBS 5%, 1% BSA) and labeled at 4°C for 15 min with the following human specific antibodies: CD34 PB (1:40; #343512), CD38 PE/Cy5 (1:40; #303507), CD90 AF700 (1:40; #328119), CD133 PE (1:10; #372803), CD184 (CXCR4) APC/Cy7 (1:40; #306527) (all from BioLegend); CD45RA APC-H7 (1:20; #560674; BD Pharmingen). Cells from BM, spleen, and thymus were analyzed by flow cytometry upon re-suspension in blocking solution (PBS 5% FBS, 1% BSA) and labeling at 4°C for 15 min with the following specific antibodies: CD13 PE (1:40; #555394), CD3 V500 (1:20; #561416), CD19 PE/Cy7 (1:80; #557835), mCD45 APC (1:100; #561018) (all BD Biosciences), and Pacific Blue anti-human CD45 (1:40; #368540; BioLegend). For the exclusion of death cells, we used either 7-AAD (1 mg/mL) or DAPI (Sigma-Aldrich). Cells were analyzed using the LSR Fortessa instrument or sorted using the BD FACSAria III Cell Sorter (Becton Dickinson, Franklin Lakes, NJ) at the Flow Cytometry Sorting Facility of Dana-Farber Cancer Institute.

LV integration retrieval and analysis

Briefly, LTR vector-genome junctions were amplified by restriction-based LM-PCR.²² gDNA (1 μ g) was digested overnight at 37°C with the Tru91 restriction enzyme (Roche), purified by NucleoSpin Gel and PCR Clean-up kit (MACHEREY-NAGEL), and ligated overnight to a TA-protruding double-stranded DNA linker by T4 DNA Ligase (New England Biolabs), as previously described.²² Ligated DNA was purified, digested overnight at 37°C with SacI (Roche), and purified again. Multiple nested PCRs (10–20) were performed with specific primers annealing to the linker and the vector LTR, adapted to Illumina sequencing and containing a 4 bp sample-specific barcode for sample identification. Libraries were quantified on NanoDrop 2000 Spectrophotometer (Thermo Fisher Scientific) and loaded on a 1% agarose gel for amplicon size selection. Amplicons ranging from 200 to 500 kb were manually extracted from the gel and purified using NucleoSpin Gel and PCR Clean-up kit. About 1 μ g of the final libraries were subsequently processed with MiSeq Reagent Kit version 3 (2 \times 300 bp pair-end sequencing) following the manufacturer's instructions, bar-coded with a 6 bp sample-specific tag, and sequenced to saturation on an Illumina MiSeq machine at IGA Technology Services (Udine, Italy). Raw reads resulting from Illumina paired-end sequencing were bioinformatically trimmed to recover the human genome sequences adjacent to the proviral LTR, as previously described,³⁵ and mapped on the reference genome (human NCBI Hg38) using the BWA-MEM software (>95% identity).³⁶ The genomic coordinates of the first nucleotide in the host genome adjacent to the viral LTR were indicated as ISs. ISs originated by different reads mapping in the same genomic position were collapsed recovering the number of corresponding reads (read count). Unique ISs were annotated on the RefSeq gene database as intergenic or

intrinsic (exonic or intronic). Genes (defined by the most upstream transcription start site to the most downstream end) hosting at least one IS were identified as target genes. The threshold to define the top 1% most targeted genes was defined as the 0.99 percentile of the gene targeting score (number of ISs falling inside a gene body). Biological function enrichment in the list of LV target genes was assessed with the statistical overrepresentation test and statistical enrichment test of the Gene Ontology Resources software available at <http://geneontology.org> on the basis of the PANTHER knowledgebase classification system.³⁷ Cancer Gene List³⁸ was obtained from Bushman Laboratory (University of Pennsylvania, Philadelphia) at <http://www.bushmanlab.org/links/genelists>.

Statistical analysis

Student's t test or ANOVA with multiple pairwise comparisons was used to compare two or more groups, while the chi-square statistic was used to compare frequencies, unless differently indicated in the figure legends. Differences were considered statistically significant at values of * $p < 0.05$, ** $p < 0.01$, *** $p < 0.001$, and **** $p < 0.0001$. In all figures with error bars, the graphs depict mean (SD) unless otherwise indicated in the figure legend.

DATA AND CODE AVAILABILITY

Additional data are available upon request to the corresponding authors.

SUPPLEMENTAL INFORMATION

Supplemental information can be found online at <https://doi.org/10.1016/j.omtm.2023.101131>.

ACKNOWLEDGMENTS

We thank Francesca Bertolini (University of Modena and Reggio Emilia, Modena, Italy) for her contribution to LM-PCR library preparation. This work was funded by the Start-up package funds to A.B.

AUTHOR CONTRIBUTIONS

Study design, V.P., A.M., and A.B.; study execution, V.P., A.M., and D.P.; data analysis, V.P., A.M., D.P., and A.B.; manuscript drafting, V.P., A.M., D.P., and A.B.; manuscript review, discussion, and finalization, V.P. and A.B.

DECLARATION OF INTERESTS

The authors declare no competing interests.

REFERENCES

- Hoggatt, J., and Pelus, L.M. (2010). Eicosanoid regulation of hematopoiesis and hematopoietic stem and progenitor trafficking. *Leukemia* 24, 1993–2002. <https://doi.org/10.1038/leu.2010.216>.
- North, T.E., Goessling, W., Walkley, C.R., Lengerke, C., Kopani, K.R., Lord, A.M., Weber, G.J., Bowman, T.V., Jang, I.H., Grosser, T., et al. (2007). Prostaglandin E2 regulates vertebrate hematopoietic stem cell homeostasis. *Nature* 447, 1007–1011. <https://doi.org/10.1038/nature05883>.
- Hoggatt, J., Singh, P., Sampath, J., and Pelus, L.M. (2009). Prostaglandin E2 enhances hematopoietic stem cell homing, survival, and proliferation. *Blood* 113, 5444–5455. <https://doi.org/10.1182/blood-2009-01-201335>.
- Cutler, C., Multani, P., Robbins, D., Kim, H.T., Le, T., Hoggatt, J., Pelus, L.M., Despoints, C., Chen, Y.B., Rezner, B., et al. (2013). Prostaglandin-modulated umbilical cord blood hematopoietic stem cell transplantation. *Blood* 122, 3074–3081. <https://doi.org/10.1182/blood-2013-05-503177>.
- Hoggatt, J., Mohammad, K.S., Singh, P., and Pelus, L.M. (2013). Prostaglandin E2 enhances long-term repopulation but does not permanently alter inherent stem cell competitiveness. *Blood* 122, 2997–3000. <https://doi.org/10.1182/blood-2013-07-515288>.
- Frisch, B.J., Porter, R.L., Gigliotti, B.J., Olm-Shipman, A.J., Weber, J.M., O'Keefe, R.J., Jordan, C.T., and Calvi, L.M. (2009). In vivo prostaglandin E2 treatment alters the bone marrow microenvironment and preferentially expands short-term hematopoietic stem cells. *Blood* 114, 4054–4063. <https://doi.org/10.1182/blood-2009-03-205823>.
- Heffner, G.C., Bonner, M., Christiansen, L., Pierciey, F.J., Campbell, D., Smurnyy, Y., Zhang, W., Hamel, A., Shaw, S., Lewis, G., et al. (2018). Prostaglandin E2 Increases Lentiviral Vector Transduction Efficiency of Adult Human Hematopoietic Stem and Progenitor Cells. *Mol. Ther.* 26, 320–328. <https://doi.org/10.1016/j.ymthe.2017.09.025>.
- Zonari, E., Desantis, G., Petrillo, C., Boccalatte, F.E., Lidonnici, M.R., Kajaste-Rudnitski, A., Aiuti, A., Ferrari, G., Naldini, L., and Gentner, B. (2017). Efficient Ex Vivo Engineering and Expansion of Highly Purified Human Hematopoietic Stem and Progenitor Cell Populations for Gene Therapy. *Stem Cell Rep.* 8, 977–990. <https://doi.org/10.1016/j.stemcr.2017.02.010>.
- Masiuk, K.E., Zhang, R., Osborne, K., Hollis, R.P., Campo-Fernandez, B., and Kohn, D.B. (2019). PGE2 and Poloxamer Synperonic F108 Enhance Transduction of Human HSPCs with a beta-Globin Lentiviral Vector. *Mol. Ther. Methods Clin. Dev.* 13, 390–398. <https://doi.org/10.1016/j.omtm.2019.03.005>.
- Lewis, G., Christiansen, L., McKenzie, J., Luo, M., Pasackow, E., Smurnyy, Y., Harrington, S., Gregory, P., Veres, G., Negre, O., and Bonner, M. (2018). Staurosporine Increases Lentiviral Vector Transduction Efficiency of Human Hematopoietic Stem and Progenitor Cells. *Mol. Ther. Methods Clin. Dev.* 9, 313–322. <https://doi.org/10.1016/j.omtm.2018.04.001>.
- Schott, J.W., León-Rico, D., Ferreira, C.B., Buckland, K.F., Santilli, G., Armant, M.A., Schambach, A., Cavazza, A., and Thrasher, A.J. (2019). Enhancing Lentiviral and Alpharetroviral Transduction of Human Hematopoietic Stem Cells for Clinical Application. *Mol. Ther. Methods Clin. Dev.* 14, 134–147. <https://doi.org/10.1016/j.omtm.2019.05.015>.
- Locatelli, F., Thompson, A.A., Kwiatkowski, J.L., Porter, J.B., Thrasher, A.J., Hongeng, S., Sauer, M.G., Thuret, I., Lal, A., Algeri, M., et al. (2022). Betibeglogene Autotemcel Gene Therapy for Non-beta(0)/beta(0) Genotype beta-Thalassemia. *N. Engl. J. Med.* 386, 415–427. <https://doi.org/10.1056/NEJMoa2113206>.
- Kanter, J., Walters, M.C., Krishnamurti, L., Mapara, M.Y., Kwiatkowski, J.L., Rifkin-Zenenberg, S., Aygun, B., Kasow, K.A., Pierciey, F.J., Jr., Bonner, M., et al. (2022). Biologic and Clinical Efficacy of LentiGlobin for Sickle Cell Disease. *N. Engl. J. Med.* 386, 617–628. <https://doi.org/10.1056/NEJMoa2117175>.
- Gentner, B., Tucci, F., Galimberti, S., Fumagalli, F., De Pellegrin, M., Silvani, P., Camesasca, C., Pontesilli, S., Darin, S., Ciotti, F., et al. (2021). Hematopoietic Stem- and Progenitor-Cell Gene Therapy for Hurler Syndrome. *N. Engl. J. Med.* 385, 1929–1940. <https://doi.org/10.1056/NEJMoa2106596>.
- Kanter, J., Thompson, A.A., Pierciey, F.J., Jr., Hsieh, M., Uchida, N., Leboulch, P., Schmidt, M., Bonner, M., Guo, R., Miller, A., et al. (2023). Lovo-cel gene therapy for sickle cell disease: Treatment process evolution and outcomes in the initial groups of the HGB-206 study. *Am. J. Hematol.* 98, 11–22. <https://doi.org/10.1002/ajh.26741>.
- Bonner, M., Kanter, J., Macari, E., Lane, R., Lewis, G., Coles, P., Kassenaar, S., Mynampati, S., Schulze, R., Hebert, M., et al. (2019). The Relationships between Target Gene Transduction, Engraftment of HSCs and RBC Physiology in Sickle Cell Disease Gene Therapy. *Blood* 134, 206. <https://doi.org/10.1182/blood-2019-129124>.
- Biffi, A., Montini, E., Lorioli, L., Cesani, M., Fumagalli, F., Plati, T., Baldoli, C., Martino, S., Calabria, A., Canale, S., et al. (2013). Lentiviral hematopoietic stem cell gene therapy benefits metachromatic leukodystrophy. *Science* 341, 1233158. <https://doi.org/10.1126/science.1233158>.
- Sessa, M., Lorioli, L., Fumagalli, F., Acquati, S., Redaelli, D., Baldoli, C., Canale, S., Lopez, I.D., Morena, F., Calabria, A., et al. (2016). Lentiviral hematopoietic stem-cell gene

- therapy in early-onset metachromatic leukodystrophy: an ad-hoc analysis of a non-randomised, open-label, phase 1/2 trial. *Lancet* 388, 476–487. [https://doi.org/10.1016/S0140-6736\(16\)30374-9](https://doi.org/10.1016/S0140-6736(16)30374-9).
19. Fumagalli, F., Calbi, V., Natali Sora, M.G., Sessa, M., Baldoli, C., Rancoita, P.M.V., Ciotti, F., Sarzana, M., Frascini, M., Zamboni, A.A., et al. (2022). Lentiviral haematopoietic stem-cell gene therapy for early-onset metachromatic leukodystrophy: long-term results from a non-randomised, open-label, phase 1/2 trial and expanded access. *Lancet* 399, 372–383. [https://doi.org/10.1016/S0140-6736\(21\)02017-1](https://doi.org/10.1016/S0140-6736(21)02017-1).
 20. Peviani, M., Das, S., Patel, J., Jno-Charles, O., Kumar, R., Zguro, A., Mathews, T.D., Cabras, P., Milazzo, R., Cavalca, E., et al. (2023). An innovative hematopoietic stem cell gene therapy approach benefits CLN1 disease in the mouse model. *EMBO Mol. Med.* 15, e15968. <https://doi.org/10.15252/emmm.202215968>.
 21. Carnec, X., Quan, L., Olson, W.C., Hazan, U., and Dragic, T. (2005). Anti-CXCR4 monoclonal antibodies recognizing overlapping epitopes differ significantly in their ability to inhibit entry of human immunodeficiency virus type 1. *J. Virol.* 79, 1930–1933. <https://doi.org/10.1128/JVI.79.3.1930-1933.2005>.
 22. Poletti, V., Charrier, S., Corre, G., Gjata, B., Vignaud, A., Zhang, F., Rothe, M., Schambach, A., Gaspar, H.B., Thrasher, A.J., and Mavilio, F. (2018). Preclinical Development of a Lentiviral Vector for Gene Therapy of X-Linked Severe Combined Immunodeficiency. *Mol. Ther. Methods Clin. Dev.* 9, 257–269. <https://doi.org/10.1016/j.omtm.2018.03.002>.
 23. Poletti, V., Urbinati, F., Charrier, S., Corre, G., Hollis, R.P., Campo Fernandez, B., Martin, S., Rothe, M., Schambach, A., Kohn, D.B., and Mavilio, F. (2018). Pre-clinical Development of a Lentiviral Vector Expressing the Anti-sickling β AS3 Globin for Gene Therapy for Sickle Cell Disease. *Mol. Ther. Methods Clin. Dev.* 11, 167–179. <https://doi.org/10.1016/j.omtm.2018.10.014>.
 24. Lidonnici, M.R., Palcari, Y., Tiboni, F., Mandelli, G., Rossi, C., Vezzoli, M., Aprile, A., Lederer, C.W., Ambrosi, A., Chanut, F., et al. (2018). Multiple Integrated Non-clinical Studies Predict the Safety of Lentivirus-Mediated Gene Therapy for β -Thalassemia. *Mol. Ther. Methods Clin. Dev.* 11, 9–28. <https://doi.org/10.1016/j.omtm.2018.09.001>.
 25. Mi, H., Muruganujan, A., Ebert, D., Huang, X., and Thomas, P.D. (2019). PANTHER version 14: more genomes, a new PANTHER GO-slim and improvements in enrichment analysis tools. *Nucleic Acids Res.* 47, D419–D426. <https://doi.org/10.1093/nar/gky1038>.
 26. Aiuti, A., Biasco, L., Scaramuzza, S., Ferrua, F., Cicalese, M.P., Baricordi, C., Dionisio, F., Calabria, A., Giannelli, S., Castiello, M.C., et al. (2013). Lentiviral hematopoietic stem cell gene therapy in patients with Wiskott-Aldrich syndrome. *Science* 341, 1233151. <https://doi.org/10.1126/science.1233151>.
 27. Hacein-Bey Abina, S., Gaspar, H.B., Blondeau, J., Caccavelli, L., Charrier, S., Buckland, K., Picard, C., Six, E., Himoudi, N., Gilmour, K., et al. (2015). Outcomes following gene therapy in patients with severe Wiskott-Aldrich syndrome. *JAMA* 313, 1550–1563. <https://doi.org/10.1001/jama.2015.3253>.
 28. Cartier, N., Hacein-Bey-Abina, S., Bartholomae, C.C., Veres, G., Schmidt, M., Kutschera, I., Vidaud, M., Abel, U., Dal-Cortivo, L., Caccavelli, L., et al. (2009). Hematopoietic stem cell gene therapy with a lentiviral vector in X-linked adrenoleukodystrophy. *Science* 326, 818–823. <https://doi.org/10.1126/science.1171242>.
 29. Fabregat, A., Sidiropoulos, K., Viteri, G., Forner, O., Marin-Garcia, P., Arnau, V., D'Eustachio, P., Stein, L., and Hermjakob, H. (2017). Reactome pathway analysis: a high-performance in-memory approach. *BMC Bioinf.* 18, 142. <https://doi.org/10.1186/s12859-017-1559-2>.
 30. Gao, J.L., Owusu-Ansah, A., Paun, A., Beacht, K., Yim, E., Siwicki, M., Yang, A., Liu, Q., McDermott, D.H., and Murphy, P.M. (2019). Low-level Cxcr4-haploinsufficient HSC engraftment is sufficient to correct leukopenia in WHIM syndrome mice. *JCI Insight* 4, e132140. <https://doi.org/10.1172/jci.insight.132140>.
 31. Mantel, C.R., O'Leary, H.A., Chitteti, B.R., Huang, X., Cooper, S., Hangoc, G., Brustovetsky, N., Srour, E.F., Lee, M.R., Messina-Graham, S., et al. (2015). Enhancing Hematopoietic Stem Cell Transplantation Efficacy by Mitigating Oxygen Shock. *Cell* 161, 1553–1565. <https://doi.org/10.1016/j.cell.2015.04.054>.
 32. Kollet, O., Petit, I., Kahn, J., Samira, S., Dar, A., Peled, A., Deutsch, V., Gunetti, M., Piacibello, W., Nagler, A., and Lapidot, T. (2002). Human CD34(+)CXCR4(-) sorted cells harbor intracellular CXCR4, which can be functionally expressed and provide NOD/SCID repopulation. *Blood* 100, 2778–2786. <https://doi.org/10.1182/blood-2002-02-0564>.
 33. Peviani, M., Das, S., Patel, J., Jno-Charles, O., Kumar, R., Zguro, A., Mathews, T.D., Milazzo, R., Cavalca, E., Poletti, V., and Biffi, A. (2022). An innovative hematopoietic stem cell gene therapy approach benefits CLN1 disease in the mouse model. Preprint at bioRxiv. <https://doi.org/10.1101/2022.03.03.482460>.
 34. McIntosh, B.E., Brown, M.E., Duffin, B.M., Maufort, J.P., Vereide, D.T., Slukvin, I.I., and Thomson, J.A. (2015). Nonirradiated NOD.B6.SCID Il2rgamma-/- Kit(W41/W41) (NBSGW) mice support multilineage engraftment of human hematopoietic cells. *Stem Cell Rep.* 4, 171–180. <https://doi.org/10.1016/j.stemcr.2014.12.005>.
 35. Biasco, L., Pellin, D., Scala, S., Dionisio, F., Basso-Ricci, L., Leonardelli, L., Scaramuzza, S., Baricordi, C., Ferrua, F., Cicalese, M.P., et al. (2016). In Vivo Tracking of Human Hematopoiesis Reveals Patterns of Clonal Dynamics during Early and Steady-State Reconstitution Phases. *Cell Stem Cell* 19, 107–119. <https://doi.org/10.1016/j.stem.2016.04.016>.
 36. Li, H., and Durbin, R. (2010). Fast and accurate long-read alignment with Burrows-Wheeler transform. *Bioinformatics* 26, 589–595. <https://doi.org/10.1093/bioinformatics/btp698>.
 37. Mi, H., Muruganujan, A., Huang, X., Ebert, D., Mills, C., Guo, X., and Thomas, P.D. (2019). Protocol Update for large-scale genome and gene function analysis with the PANTHER classification system (v.14.0). *Nat. Protoc.* 14, 703–721. <https://doi.org/10.1038/s41596-019-0128-8>.
 38. Sadelain, M., Papapetrou, E.P., and Bushman, F.D. (2011). Safe harbours for the integration of new DNA in the human genome. *Nat. Rev. Cancer* 12, 51–58. <https://doi.org/10.1038/nrc3179>.